Proceedings of the 15th International Heat Transfer Conference, IHTC-15
August 10-15, 2014, Kyoto, Japan

IHTC15-8965

EXPERIMENTAL INVESTIGATION OF THE HEAT TRANSFER PROCESS AT A GAS-DYNAMIC METHOD OF ENERGY SEPARATION

Andrey G. Zditovets[1*], Urii A. Vinogradov.[1], Alexander A. Titov[2]

[1]Institute of Mechanics, Lomonosov Moscow State University, 1, Michurinsky Pr., Moscow, 119192, Russia
[1]Institute of Mechanics, Lomonosov Moscow State University, 1, Michurinsky Pr., Moscow, 119192, Russia
[2]Open joint-stock company "Orgenergogaz", 11, Luganskaya St., Moscow, 115304, Russia

ABSTRACT

"Energy separation" is the re-distribution of the total energy (temperature) in a fluid without external work or heat. The results of an experimental investigation of the gas-dynamic method of energy separation of a supersonic air flow are presented. It is shown that in an axisymmetric supersonic channel the presence of a central body in the form of a cylindrical tube consisting of impermeable and permeable sections leads to the redistribution of the total energy of the flow. At the central body exit the mass-mean stagnation temperature of the air increases compared with its initial temperature. Also gas-dynamic method of the energy separation is investigated more particularly in a long conical supersonic channel with an outer subsonic channel. Rise of the total temperature of the supersonic flow and reduction of the total temperature of the subsonic flow with various ratio of mass flow rate are fixed.

KEY WORDS: Heat exchanger, convection, energy separation, supersonic flow, porous media.

1. INTRODUCTION

There are many examples of the energy separation of a gas flow [1-7]. On the basis of the energy (temperature) separation phenomenon the machine-free techniques of energy separation of gas flows have been developed. The overviews of some energy separation techniques and methods can be found in [8-10] The distinctive feature of the devices based on the machine-free techniques is the absence of mechanisms powered by the gas flow, such as pistons, blades, etc. In these devices the gas does not make external work and does not take part in the heat transfer to the surrounding. Thus, a gas flow with an initial stagnation (total) temperature $T_{0\infty}$ having passed through this device is divided into as minimum two flows with the stagnation temperatures $T_{01} < T_{0\infty}$ and $T_{02} > T_{0\infty}$, that is, the energy separation of the gas flow is realized. The most widespread techniques of machine-free energy separation include the vortex and resonance methods realized in the Ranque–Hilsch vortex tubes [11-13] and the Hartmann–Sprenger resonance tubes [14-16]. At present, there are many types of these devices which have found the application in the industry [17–20]. Their advantages are the simplicity of manufacturing, high reliability, low inertia, the absence of lubrication systems, and the possibility of operating on a wide range of the working body temperatures. On the other hand, they possess a considerable shortcoming which restricts their application in thermal engines and heating plants: this is the high total pressure loss of both cold and hot flows. In [21] a new method of the machine-free energy separation of a gas flow was proposed; in this method at the device exit the total pressure is almost conserved for one of two flows. The basic diagram of a machine-free energy separation device realizing this method is presented in Fig. 1.The compressed gas (air, vapor, gas mixture, etc.) supply is taken from the settling chamber 1 with the stagnation parameters $T_{0\infty}$ and $P_{0\infty}$ into the working section, where it is divided by partition *2* into two flows *3* and *4*. Flow *3* is not subjected to the geometric effect and remains subsonic, while flow *4* is accelerated in nozzle *5* up to a supersonic velocity.

*Corresponding Author: zditovets@mail.ru

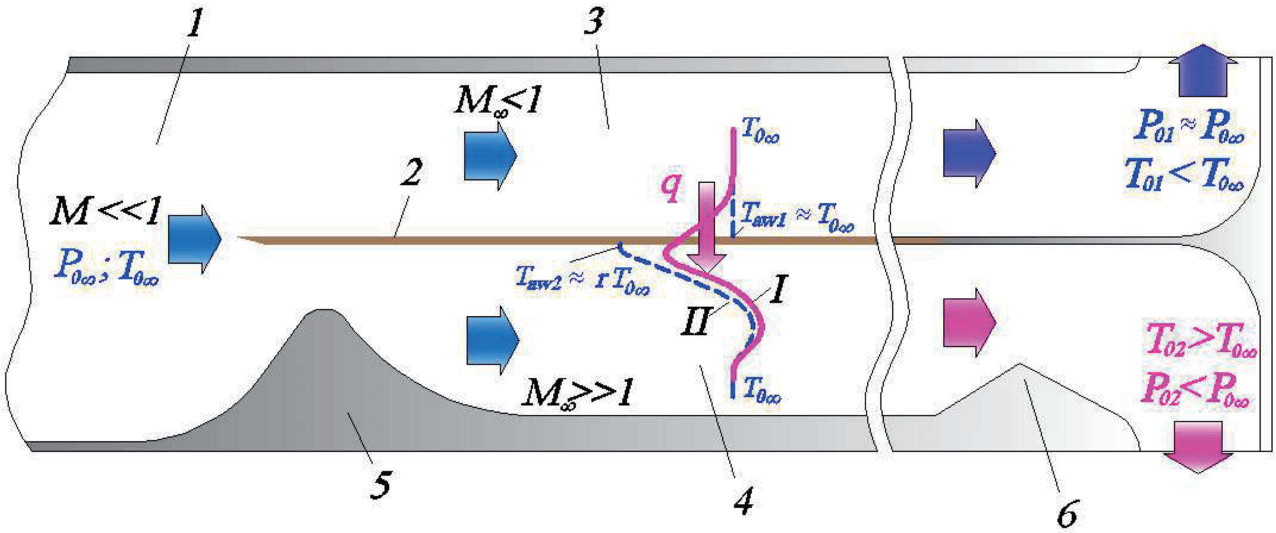

Fig. 1 Basic diagram of a device for machine-free energy separation of a flow using the gas-dynamic method [21]; (*1*) settling chamber; (*2*) separating partition; (*3*) subsonic flow; (*4*) supersonic flow; (*5*) supersonic nozzle; and (*6*) supersonic diffuser. Stagnation temperature distribution in the boundary layer in the cases of heat-conducting (*I*) and thermally-insulated (*II*) partitions.

It is known [22] that the temperature of a thermally insulated plane wall (adiabatic wall temperature) in a gas flow is determined by the expression

$$T_{aw} = \frac{T_{0\infty}\left(1 + r\dfrac{(\gamma-1)}{2}\mathrm{M}_{\infty}^{2}\right)}{1 + \dfrac{(\gamma-1)}{2}\mathrm{M}_{\infty}^{2}} \tag{1}$$

In the case of a subsonic flow ($\mathrm{M}_\infty << 1$) from Eq. (1) it follows that $T_{aw} \approx T_{0\infty}$, while in the supersonic case ($\mathrm{M}_\infty >> 1$) it can be taken that $T_{aw} \approx rT_{0\infty}$. In Fig. 1 the broken curve presents the stagnation temperature profiles in the boundary layers of supersonic and subsonic flows (partition 2 is a flat thermally insulated plate and $r < 1$). The partition surface temperatures on the subsonic (T_{aw1}) and supersonic (T_{aw2}) flow sides are different. Therefore, if the partition is made heat-conducting, then the heat transfer between the two flows begins. In this case, the supersonic flow is heated and the subsonic flow is cooled. In this device $T_{aw} \approx rT_{0\infty}$ is the greatest, theoretically permissible temperature of the subsonic flow cooling. If $r > 1$, then the heat flux is directed in the opposite direction. At $r = 1$ the heat transfer between the two flows is absent and energy separation does not occur. The specific heat flux is determined by the expression

$$\dot{q} = \frac{(T_{aw1} - T_{aw2})}{\dfrac{1}{\alpha_1} + \dfrac{\delta}{k} + \dfrac{1}{\alpha_2}} = \frac{1}{\dfrac{1}{\alpha_1} + \dfrac{\delta}{k} + \dfrac{1}{\alpha_2}}(1-r)T_{0\infty} \tag{2}$$

We will consider in more detail the methods of influencing the temperature recovery factor which could be applied for enhancing the energy (temperature) separation in the device under consideration.

From the approximation of the exact solution of equations of the laminar compressible gas boundary layer on a flat plate it follows that $r = \sqrt{\mathrm{Pr}}$ [22]. For the turbulent boundary layer on a flat plate $r = \sqrt[3]{\mathrm{Pr}}$. In case of the turbulent boundary layer on a flat plate and air as a working gas (Pr=0.72) $r \approx 0.9$.

As shown in [23–25], the application of a surface relief (holes, grooves, annular protrusions, notches, etc.) on a plate leads to a reduction of the surface-average temperature recovery factor. Depending on the surface relief the local values of r can vary within the limits from 0.82 to 0.91 and the surface-average values from 0.85 to 0.87; thus, one of the means of enhancing the energy (temperature) separation is the application of the surface relief on the partition *2* (Fig. 1) on the supersonic flow side.

The temperature recovery factor can be very considerably reduced on a porous permeable surface through which gas is blown into a supersonic boundary layer. The most known experimental results are presented in Fig. 2 [26]. In this figure the temperature recovery factor is plotted against the injection parameter $b_M = j/St_M$, Clearly, gas injection into a supersonic boundary layer can lead to a considerable reduction in the temperature recovery factor r on the permeable plate as compared with the impermeable plate.

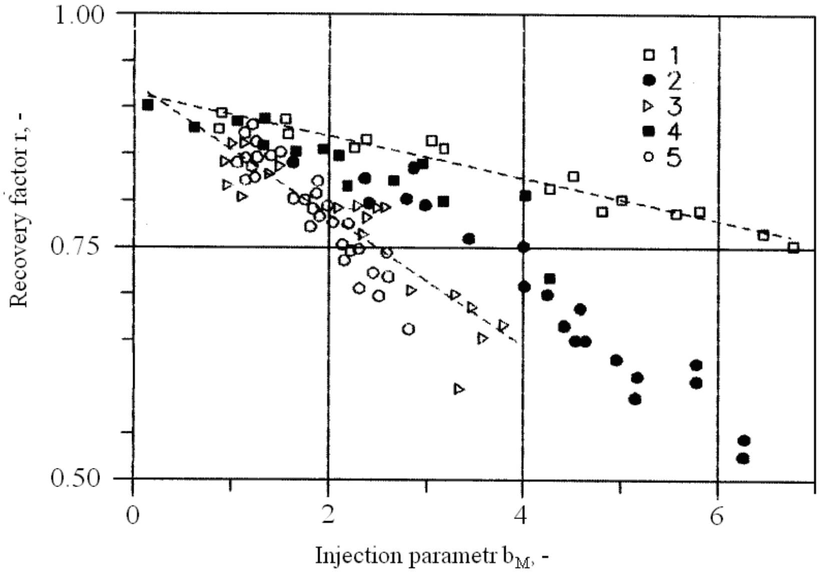

Fig. 2 Experimental dependence of the temperature recovery factor r on the injection parameter $b_M = j/\mathrm{St}_M$; (1) [27], M = 3.2; (2) [28], M = 2.5; (3) [29], M = 2.3; (4) [30], M = 3; and (5) [31], M = 2.7; broken lines approximate the experimental data

The gas injection effect on the amount of the heat transferred from the subsonic to the supersonic flow was theoretically considered in [9, 21, 32-34]. The case of an impermeable wall was theoretically considered in [9, 21, 33–38].

The purpose of this study is an experimental investigation of the energy (temperature) separation process in a device realizing the gas-dynamic method described above and the effects which occur if a porous permeable surface is used as a separating wall.

2. MODELS AND EXPERIMENTAL CONDITIONS

The experimental investigation was carried out in the hypersonic aerodynamics laboratory of the Institute of Mechanics of the Lomonosov Moscow State University.

2.1 An setup for investigation an influence of a porous media on the gas-dynamic energy separation method The working section of the experimental facility is used for the investigation of the porous permeable surface effects is schematically presented in Fig. 3. An axisymmetric contoured supersonic nozzle *1* smoothly goes over into the conical tube *2* thus forming a supersonic channel. In the study three model central bodies differing in the working section material were used; model *1* had the working section made of heat insulator (ebonite, k = 0.16 W/(m K) [39]); model *2* had a heat-conducting working section (copper tube, k= 384 W/(m K)[39]); and model *3* had a permeable tube (sintered electrocorundum, k = 40

W/(m K) [40], open porosity of 37 to 38%, the pore diameter of 60 to 65 μm, and the density of 2210 kg/m^3).

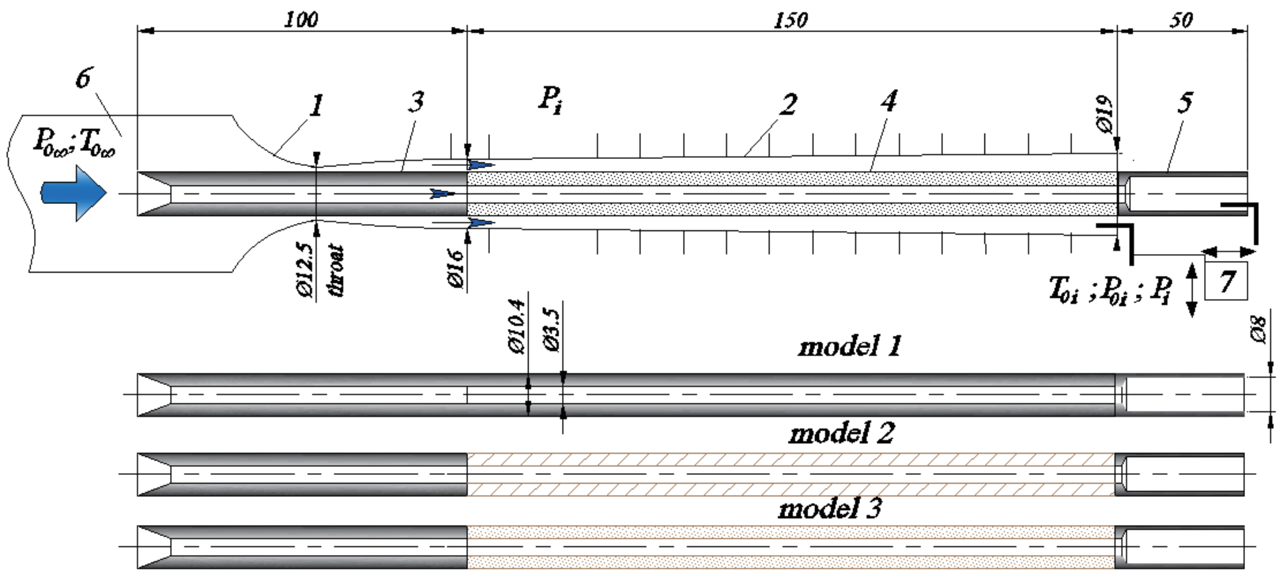

Fig. 3. Diagram of the working part of the experimental setup and the model central bodies; (*1*) supersonic contoured nozzle; (*2*) conical tube (ebonite); (*3*) impermeable tube (ebonite); (*4*) working section of the central body; (*5*) exit diffuser; (*6*) settling chamber; and (*7*) coordinate device

During the facility operation the air from the settling chamber *6* arrives to two channels; the first is the inner channel of the central body and the second is the annular channel formed by the inside surfaces of the supersonic nozzle and the conical tube and the outside surface of the central body. In the outer channel the air is accelerated to a supersonic velocity in the supersonic nozzle. At the nozzle exit the nominal Mach number M = 2.66. In the same section of the inner channel the flow remains subsonic. Then it is the material of the working section of the model central body that determines the nature of the interaction between the inner and outer flows. Thereupon the inner flow is decelerated in diffuser *5*, while the outer flow flows out directly into the atmosphere. The investigation included the following measurements. On the lateral surface of the conical tube *2* (Fig. 3) there were static pressure orifices located at 26 points (13 points on each side); one more was near the supersonic nozzle exit. In the settling chamber there were three stagnation pressure ($P_{0\infty}$) orifices and four stagnation temperature ($T_{0\infty}$) probes. The profiles of the stagnation P_{0i} and static P_i pressures and the stagnation temperature T_{0i} of the outer and inner flows were measured using special probes fastened on the coordinate device *7* (Fig. 3). A maximum depth of probe immersion amounted to 40 mm from the exit section of the conical tube. The outside diameter of the pressure probes was 1.2 mm and that of the stagnation temperature probe was 1.6 mm. The pressure was measured with the pressure transducers. The temperature measurements were carried out using chromel-nickel thermocouples. In measuring the stagnation temperature in the settling chamber the absolute random error was ±0.3°C and in measuring the stagnation temperature profile by means of the probe it was ±0.6°C. The investigation included three stages. In the first stage the central body was the heat insulator (model 1 Fig. 3). The data obtained in this case corresponded to the regime in which there is no interaction between the flows. They provided the basis for estimating the energy separation amount in the subsequent stages. In the second stage model 2 was used (Fig. 3); in this form the setup operated in some accordance with the diagram presented in Fig. 1. In the third stage the model central body included a permeable section (model 3 Fig. 3). In all the stages the stagnation parameters in the settling chamber (pressure and temperature) were maintained the same. The measurements were carried out only after a steady regime has been attained.

2.2 An setup for gas-dynamic energy separation method The working section of the experimental facility is used for more particular investigation of the gas-dynamic method of the energy separation is schematically presented in Fig. 4.

(a)

(b)

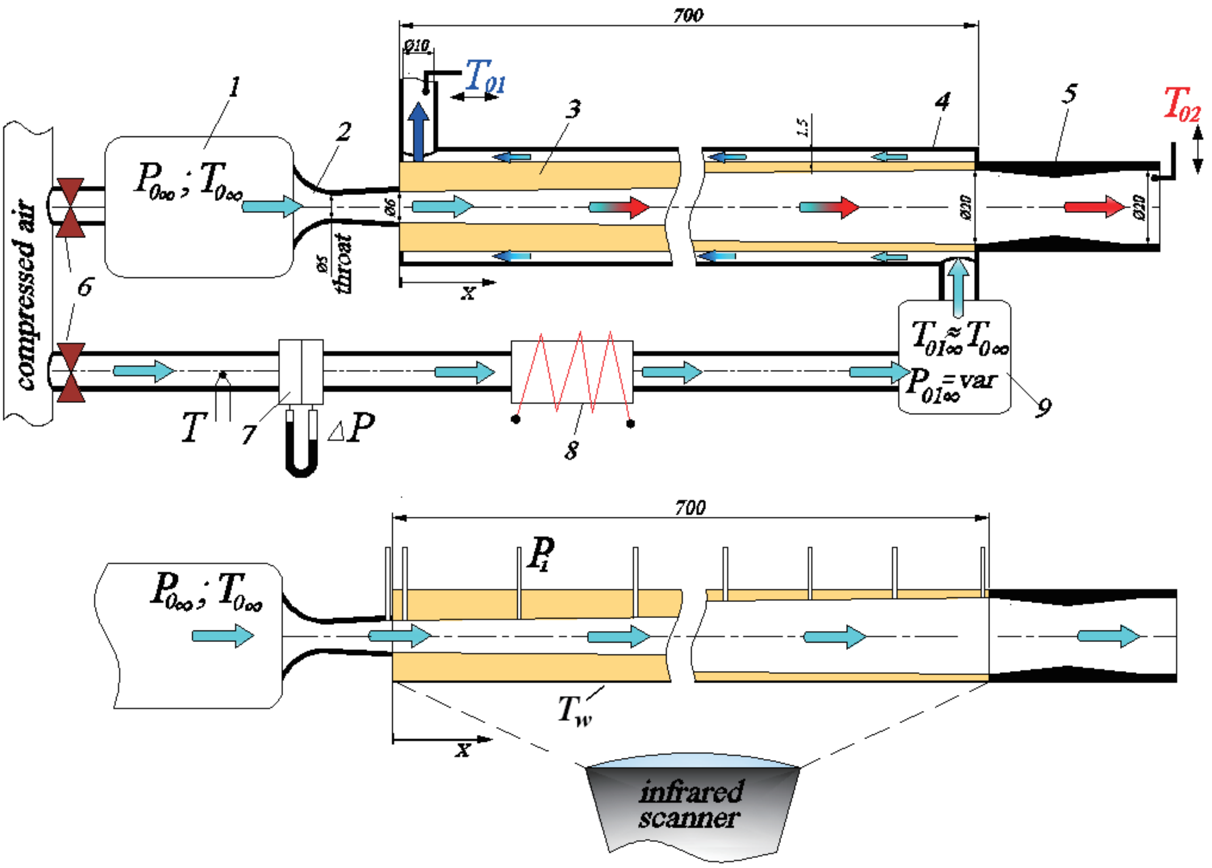

Fig. 4 Diagram of the working part of the experimental setup (a) and scheme (b) for static pressure and surface temperature measurement; (*1*) settling chamber; (*2*) supersonic conical nozzle; (*3*) conical tube (brass); (*4*) heat-insulated tube; (*5*) exit diffuser; (*6*) valves; (*7*) nozzle for mass flow measuring; (*8*) electric heater; (9) settling chamber for subsonic channel

Compressed air passed through inlet valves *6* supplies to the setup. The setup's working part consists of the supersonic and subsonic channels. The supersonic channel is formed by the axisymmetric conical supersonic nozzle *2*, the conical tube *3* and the supersonic diffuser *5*. It is connected with the settling chamber *1*. The subsonic channel is formed by the outer surface of the conical tube *3* and the inner surface of a tube *4*. The subsonic channel is supplied by air from the settling chamber *9*. The air temperature ($T_{01\infty}$) at the enter of the subsonic channel is maintained equal to the temperature at the settling chamber *1* with using of the electric heater *8*. A mass flow rate of the subsonic stream is calculated using the pressure drop in the measuring nozzle *7*. Using the valve 6 the mass flow rate through subsonic channel can be changed. A mass flow rate through supersonic channel has a constant value during the experiments and is calculated using the parameters in the settling chamber and the meaning of the critical nozzle area. At the supersonic nozzle *2* exit the nominal Mach number is M = 1.8. In the settling chamber there were three stagnation pressure ($P_{0\infty}$) probes and four stagnation temperature ($T_{0\infty}$) probes. The profiles of the stagnation temperature at the exit of the subsonic T_{01} and supersonic T_{02} flows were measured using special probes fastened on the coordinate device. The outside diameter of the stagnation temperature probes was 1.6 mm. The scheme of setup shown in Fig. 4(b) is used to measure static the distribution of the static pressure along the supersonic channel. On the lateral surface of the conical tube *3* there were static pressure orifices located at 8 points; one more head was near the supersonic nozzle exit. The measurements of the static pressure profile along the supersonic channel were carried out when tube *4* was removed. Also external surface temperature of the conical tube was measured with using an infrared scanner in the same experiment. This surface was blackened with soot. It gave us the opportunity to evaluate the lowest temperature value which we could obtain for subsonic flow with the same stagnation parameters in the settling chamber. The setup was fully assembled during temperature profile measurement and the stagnation pressure and temperature in the settling chamber *1* were maintained the same as during the static pressure profile measurement. The pressure was measured with the pressure transducers. The temperature measurements were carried out using chromel-nickel thermocouples. In measuring the stagnation temperature in the settling chamber the absolute random error was ±0.3°C and in measuring the stagnation temperature profile by means of the probe it was ±0.6°C.

3. RESULTS AND DISCUSSION

3.1 An influence of a porous media on the gas-dynamic energy separation method In Fig. 5 the stagnation temperature and Mach number profiles in the inner and outer flows are plotted for the three model central bodies. In the outer flow the measurements were performed at a distance of 7 mm from the exit section of the conical tube and in the inner flow they were carried out at a distance of 10 mm from the exit section of the central body diffuser. The Mach number profiles were calculated from the values of the total and static pressures measured by the corresponding probes at the corresponding points. In the first stage model *1* (heat insulator) was used as the central body. In this case, there was no interaction between the flows. Therefore, the mean-mass stagnation temperatures in the inner and outer channels were the same and equal to the stagnation temperature in the settling chamber. Before turning to the temperature profiles presented in Fig. 5(b) we will note the important feature concerning the stagnation temperature measurement by means of probes in a high-velocity flow. The temperature measured by the thermocouple of the probe is different from the actual stagnation temperature at this point being somewhat lower. For any particular probe design on a wide temperature range this difference depends only on the velocity of the flow past the temperature probe. In particular, the temperature presented in Fig. 5(b) is that measured by the probe rather than the actual stagnation temperature of the flow. However, in view of the fact that the Mach number distributions along the inner channel are similar in shape for all the three models Fig. 5(c), the measurements were carried out using the same probe, and the stagnation temperature range is small, it may be assumed that at each point of a cross-section the difference in the stagnation temperature, when one model was replaced by another, was fixed with a sufficient degree of accuracy. Since in the outer channel at the point of measurement of the stagnation temperature Fig. 5(a) the Mach number profiles Fig. 5(c) are considerably different for different models, in this case the conclusions on the basis of the measured data should be made with caution. In what follows, we will discuss only the temperature profiles measured at the central body exit.

The stagnation temperature in the settling chamber was 21.5 ± 0.3°C, while the mean-mass temperature measured by the probe at the model 1 exit was 18.6 ± 0.6°C. This temperature is lower than the stagnation temperature in the settling chamber in view of the reasons presented above. It was used as the reference temperature in determining the energy separation in the case of models 2 and 3. In the case of model 2 with a heat-conducting working section heat transfer between the flows arose. As can be seen in Fig. 5(b), in this case the temperature profile lies lower; therefore, the heat is removed from the flow. The mean-mass temperature was 17.2± 0.6°C. So small difference in the mean-mass temperatures is attributable to the fact that for the given heat transmission coefficient value the area of the working surface of model 2, through which the heat transfer was realized, was insufficient for achieving sufficient cooling effect. Thus, both the heat transfer area and the heat transmission coefficient must be increased in order to enhance the energy separation effect (all other things being the same). Such investigation is discussed below.

An interesting result was obtained in the case of model 3. The mean-mass temperature at the central body exit turned out to be 25.8 ± 0.6°C which is about 7°C higher than in the absence of the interaction between the flows (model 1). It was necessary to understand the reason for heating the inner flow. As shown in Fig. 2, gas injection into the supersonic flow reduces the temperature recovery factor and, therefore, a more intense heat transfer between the flows and a more considerable reduction in the temperature at the central body exit than in the case of model 2 might be anticipated [9, 21, 33].

(a)

(b)

(c)

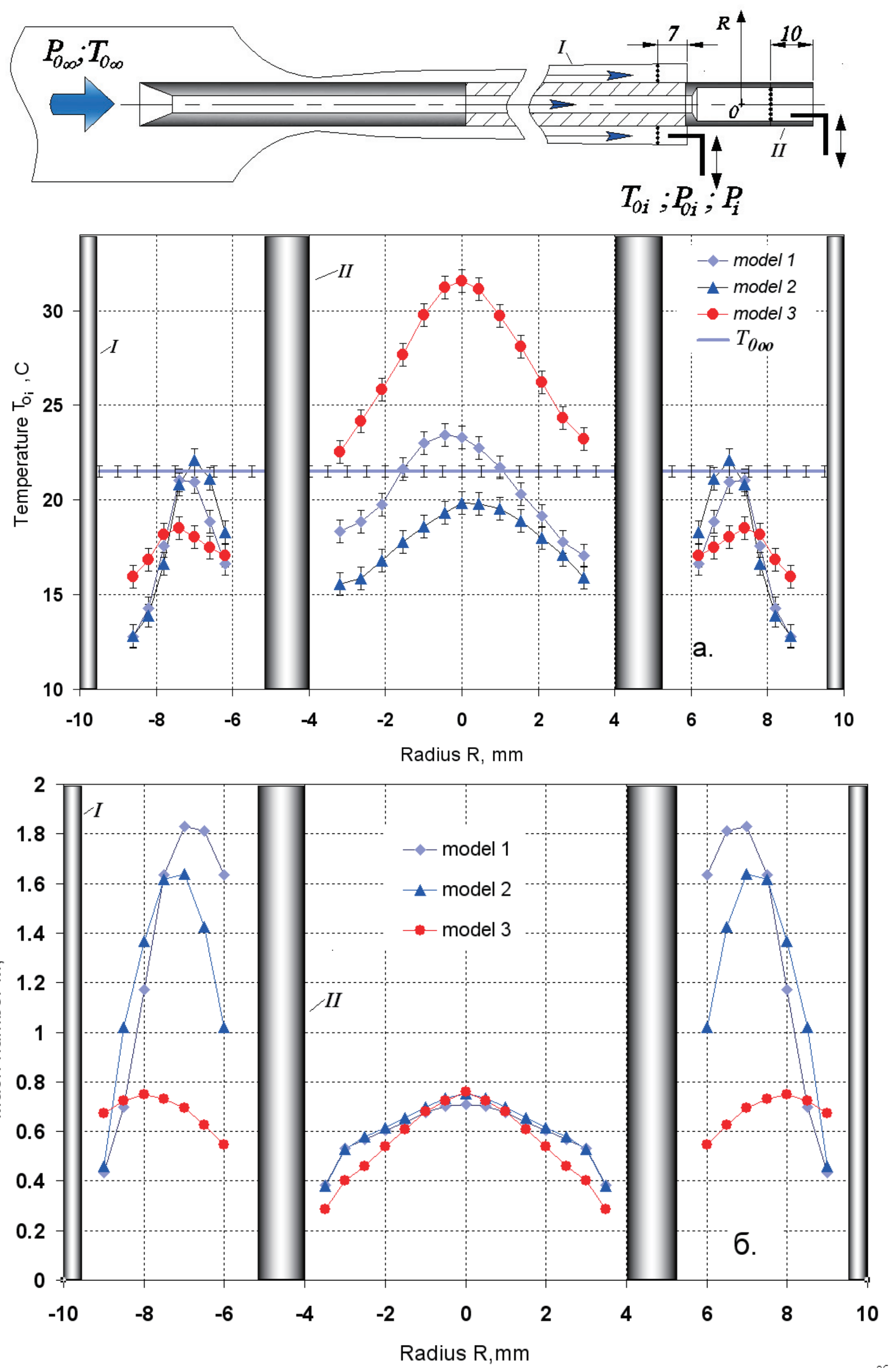

Fig. 5 Setup (a) and flow temperature (b) and Mach number (c) profiles measured at distances of 7 mm from the exit section of the outer channel (I) and 10 mm from the exit section of the exit diffuser (II); $T_{0\infty}$ = 21.5±0.3 °C.

With this in mind, we measured the total and static pressure profiles in the inner and outer channels at distances of 20 and 30 mm from the exit section of the outer channel Fig. 6(a). In this case, the central body (model 3) had no exit diffuser. The further immersion of the probe was limited by its design features. It turned out that on the measured depths the flow within the porous permeable tube is supersonic, while in the annular channel it is subsonic Fig. 6(b).

(a)

(b)

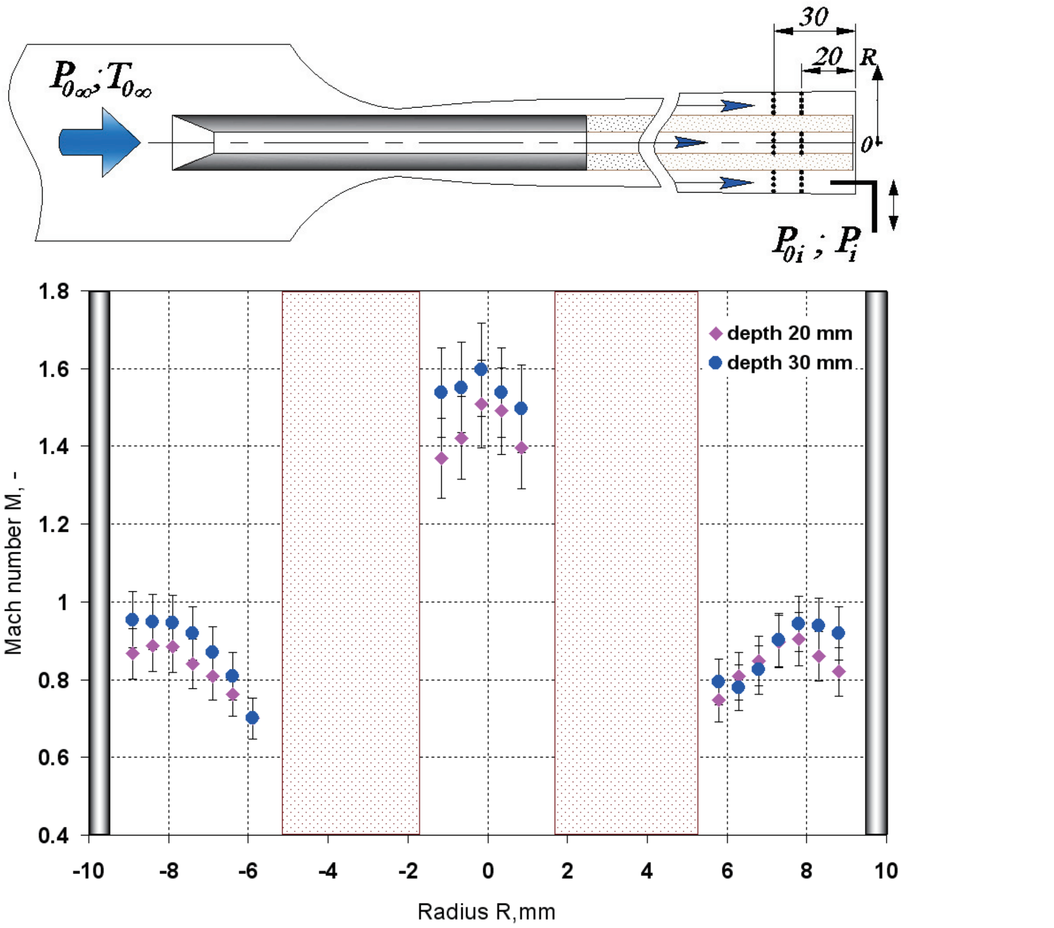

Fig. 6 Setup (a) and Mach number distribution in the cross-sections of the inner and outer channels (b); depth of 20 and 30 mm ; the central body is model *3* without the exit diffuser

The result obtained can be explained as follows. We will base on the results obtained using numerical simulation of the turbulent boundary layer on a permeable surface [34]. We will consider the integral energy relation derived on the basis of the energy equation for the stagnation enthalpy $h_0 = h + 0.5u^2$, when the gas flows along a cylindrical channel in the presence of mass transfer (injection or suction)

$$\frac{d}{dx}\int_0^{R_0} \rho u(h_0 - h_{0\infty})\frac{R}{R_0}dR = \rho v\left(h_{0\infty} - h_{0w}\right) + \frac{k}{c_p}\left(\frac{dh_0}{dR}\right)_w = \dot{q}_j - \dot{q}_w \qquad (3)$$

where R and R_0 are the current radius and the tube radius, $h_{0\infty}$ is the stagnation enthalpy in the undisturbed flow (at the tube entry), h_w is the gas stagnation enthalpy at $R = R_0$, $\dot{q}_j$ is the convective enthalpy flux, $\dot{q}_w = -\frac{k}{C_p}\left(\frac{dh_0}{dR}\right)_w$ is the diffusive heat flux to the wall. The derivation of an analogous relation in the case of a plane flow can be found in [41]. From eq. (3) it follows that a variation in the stagnation enthalpy of a gas flow h_0 that takes part in heat and mass transfer, is possible at the expense of the diffusive and convective mechanisms of the stagnation enthalpy transfer through the wall separating the interacting gas flows. The relations between these fluxes for different relative velocities of the interacting gas flows are considered in detail in [34]. The internal flow heating can be explained on the basis of the assumption that at a certain distance from the beginning of the porous section this flow acquires a velocity higher than that of the external flow, which is experimentally confirmed at x = 120 mm (depth 30 mm) Fig. 6(b). In this case, $h_{0w} < h_{0\infty}$ and the terms on the right side of eq. (3) are summed, since the diffusive heat flux is directed from the external to the internal flow. The convective enthalpy transfer favors the removal of the “cold” gas of wall layers from the boundary layer of the internal flow, thus increasing the temperature of the remaining gas. Thus, the gas suction from the inner channel not only accelerates the flow up to supersonic velocities but also favors the enhancement of the energy separation of the flows due to the addition of the diffusive and convective heat transfer mechanisms.

In Fig. 7 the static pressure distribution along the annular channel length is presented for the models of all the three types. In the case of models *1* and *2* the static pressure profile is smooth and the pressure slowly decreases to x = 120 mm. Therefore, in the region from x = −4 to x = 120 mm the air flow remains supersonic and is accelerated somewhat, that is, the effect of the channel area-of-passage expansion due to conicity is predominant over the effects of the friction work. Then, starting from x = 120 mm the flow is decelerated in a “pseudoshock” (region of supersonic-to-subsonic flow transition). This pattern, typical of supersonic flow deceleration in channels, is described in detail in [42].

(a)

(b)

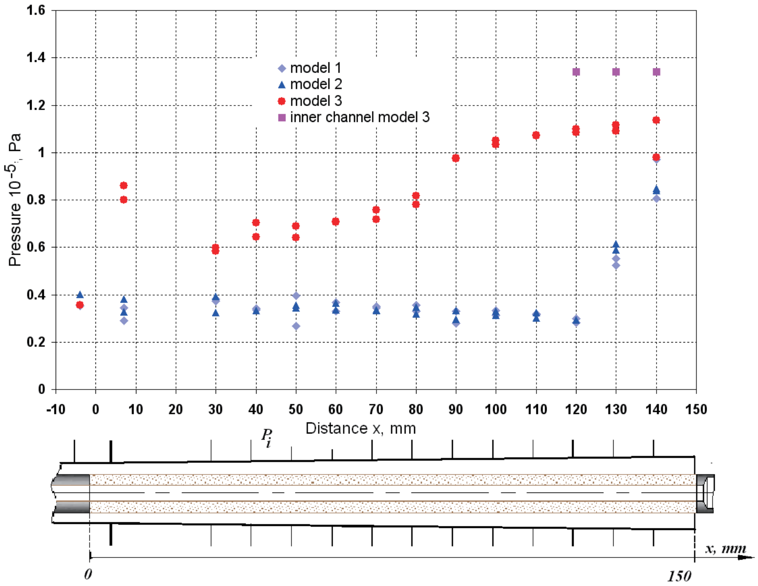

Fig. 7 Static pressure distribution (a) along the length of the outer annular channel and within the porous permeable tube (model 3); the stagnation pressure in the plenum chamber $P_{0\infty}$= 0.74 MPa; diagram of the location of the static pressure heads (b).

In the presence of the flow-rate (injection) effect (Fig. 7, model *3*) the static pressure profile considerably changes. At the point with the coordinate x = 7 mm there is a static pressure splash due to the beginning of injection into the supersonic flow and then a continuous static-pressure growth can be observable. The nature of the pressure distribution makes it possible to conclude that the supersonic flow is considerably decelerated and goes over into a subsonic flow through a “pseudoshock” on the interval from x = 60 to 100 mm. The probe measurements showed that at the point with the coordinate x = 120 mm the flow is subsonic. Thus, the mass transfer through the porous permeable region leads to flow acceleration in the inner channel up to supersonic velocities and to considerable flow deceleration in the outer annular channel. It should be noted that in the inner channel the static pressure in the probe measurement region x = 120 to 140 mm remains higher than the static pressure of the flow in the annular channel (Fig. 7). Therefore, it may be asserted that the mass transfer direction does not change when the flow in the annular channel becomes sonic. The more detailed information can be find in [43].

To provide a deeper understanding of the processes occurring during the acceleration of the gas flow moving in a channel with permeable walls in the presence of the thermal and gas-injection up to supersonic velocities an experimental investigation must be performed with large-scale models which would make it possible to obtain the local flow parameters with a high accuracy and reliability.

3.2 The results of the gas-dynamic energy separation method In Fig. 8(b) the experimental and nominal distributions of the static pressure are presented.

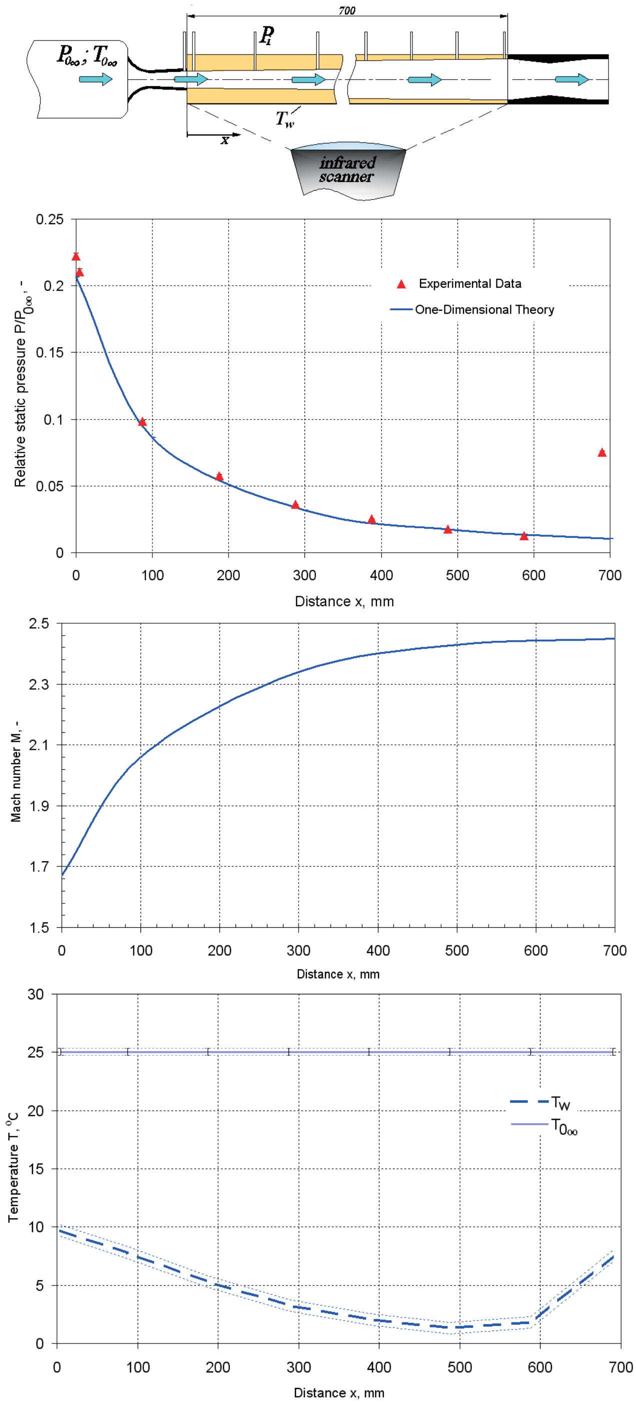

Fig. 8 Setup (a) and static pressure (b), Mach number (c) and temperature of the outer surface (d) distributions along the length of the supersonic channel; the stagnation pressure and temperature in the settling chamber $P_{0\infty}$= 1.41 MPa, $T_{0\infty}$=25±0.3 °C, G_2=0.066±0.007.

The nominal distribution of the static pressure and Mach number (Fig 8b-c) was obtained as a solution of equations for one-dimensional flow with friction and area change [44] for conditions and geometry realized in the experiments. Fig.8(c) shows a temperature of the outer surface of the supersonic channel measured with infrared devices. The raise of the static pressure and the surface temperature at the distance x = 600mm took place because of the supersonic diffuser did not work properly so the shock wave was at the exit of the supersonic channel. Still the temperature of the outer surface of the supersonic channel is lower than stagnation temperature in the settling chamber hence a stream which had a temperature equals to the stagnation temperature and a velocity much lower than supersonic one can be cooled being in contact with this surface. So the machine-free energy separation will take place.

(a)

(b)

(c)

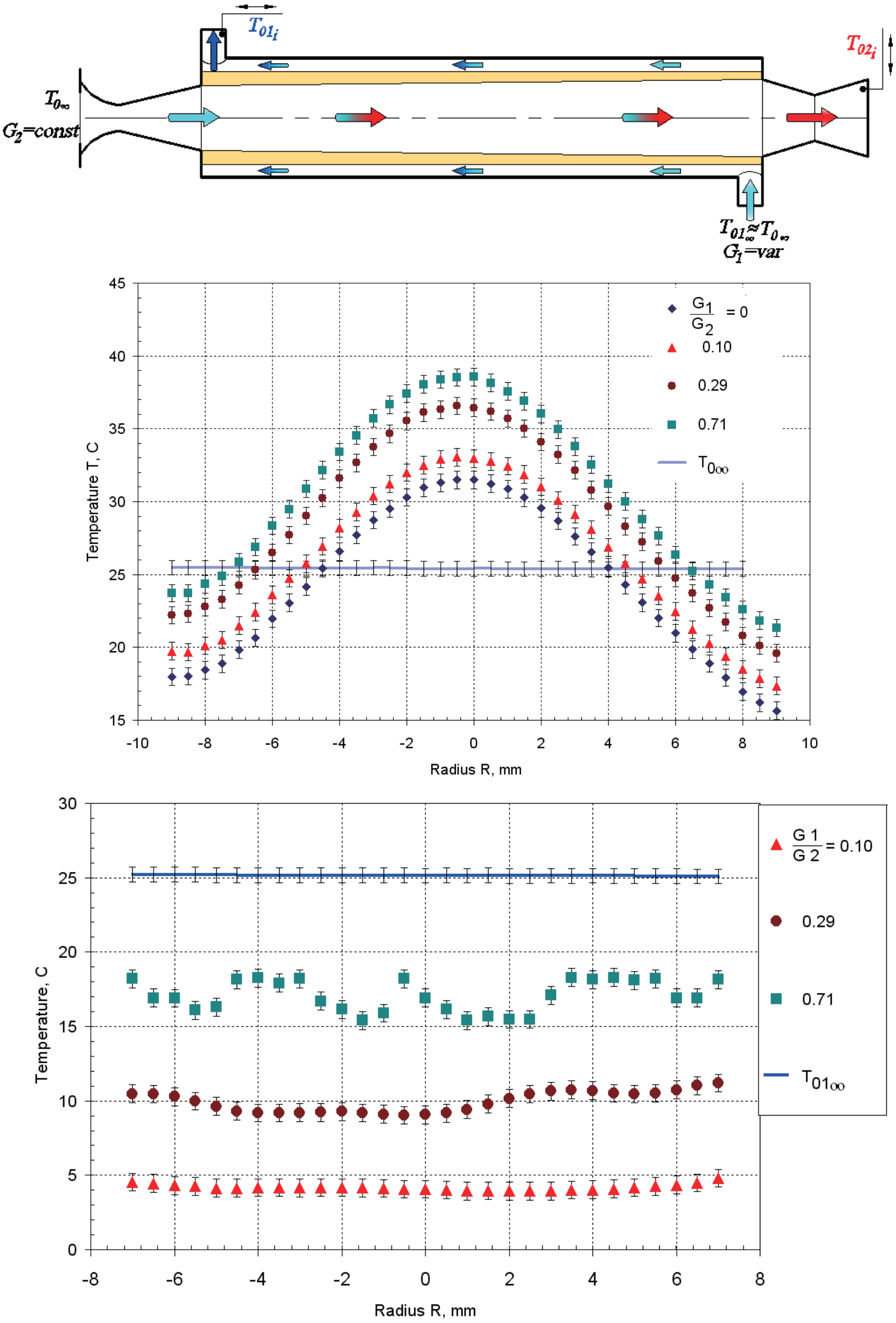

Fig.9 Setup (a) and temperature distribution measured with probes at the exit of the supersonic diffuser (a) and subsonic channel (b) for different values relative mass flow rate through subsonic channel; the stagnation pressure and temperature in the settling chamber $P_{0\infty}$= 1.41 MPa, $T_{0\infty}$= $T_{01\infty}$=25±0.3 °C, G_2=0.066±0.007.

Fig. 9(a) shows the stagnation temperature distribution measured with probes at the exit of the supersonic diffuser for different values of the relative mass flow rate through subsonic channel (the mass flow rate through supersonic channel was constant). Fig. 9(b) shows the stagnation temperature distribution measured with probes at the exit of the subsonic channel for the same values relative mass flow rate through subsonic channel. The stagnation temperatures of the air in the both settling chambers were the same throughout all experiments. As can be seen presence of the subsonic flow leads to the heating of the supersonic flow and the more is a mass flow rate of the subsonic flow the less ones temperatures differs from the initial stagnation temperature. Fig. 10 shows an absolute value of heating of the supersonic flow and an absolute value of cooling of the subsonic flow. As can be seen the regime with lowest flow rate through subsonic channel gives a maximum temperature separation effect. It should be noticed that T_{0i} in Fig.10 represent mean-area temperature of a gas flow.

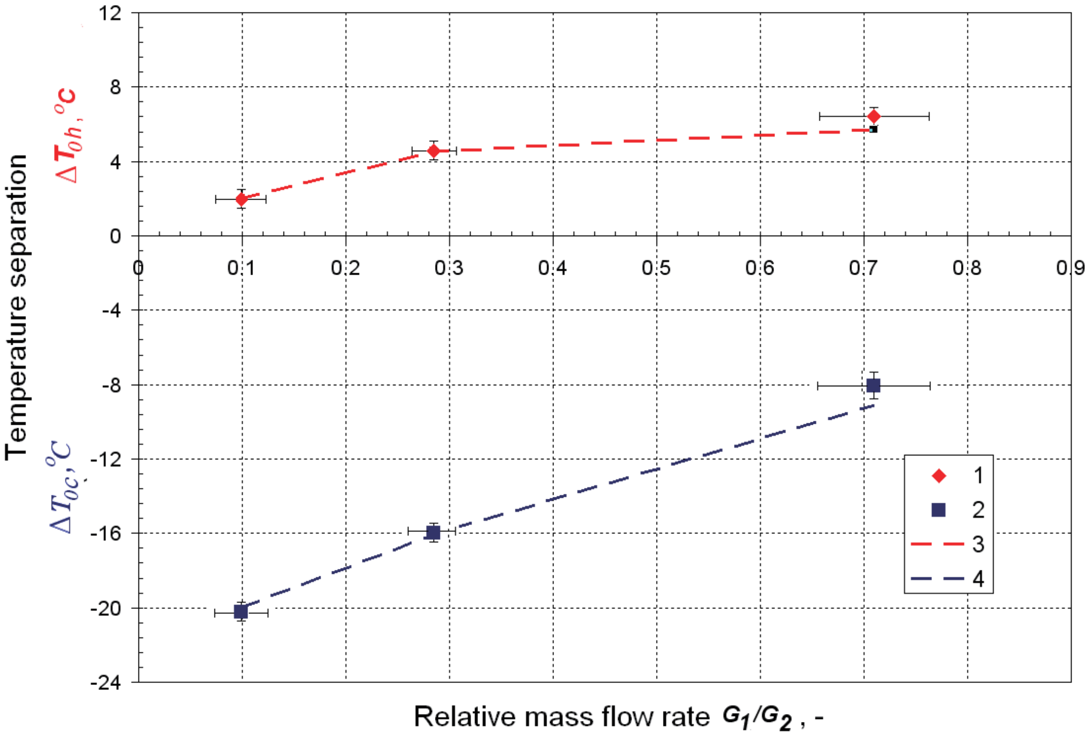

Fig. 10 An absolute value of the temperature separation with for different values relative mass flow rate through subsonic channel; the stagnation pressure and temperature in the plenum chamber $P_{0\infty}$= 1.41 MPa, $T_{0\infty}$=25±0.3 °C, G_2=0.066±0.007; (1) - T_{02}-$T_{0\infty}$ heating of the supersonic flow, (2) - T_{01}-$T_{01\infty}$ cooling of the subsonic flow, (3-4) – heat balance

6. CONCLUSIONS

A new machine-free energy separation method of an air flow was investigated experimentally. As a result of the interaction between subsonic and supersonic streams, the energy exchange between the streams occurred and the energy separation took place. The subsonic stream was cooled and the supersonic one was heated. Also it was shown that a transverse mass flow can have a significant and sometimes unexpected effect on the energy separation. The fact of the reversion of energy (temperature) separation of the streams when replacing an impermeable wall by a permeable one was established.

ACKNOWLEDGMENT

This study was supported by the Russian Foundation for Basic Research (**projects 12-08-33009**)

NOMENCLATURE

M	Mach number	(-)
St	Stanton number	(-)
T	temperature	(K)
P	pressure	(Pa)
G	mass flow rate	(kg/s)
b	injection parameter	(-)
r	recovery factor	(-)
$\dot{q}$	heat flux	(W/m^2)
k	thermal conductivity	(W/m K)
c_p	specific heat capacity	(J/kg K)
u	velocity	(m/s)
ρu	mass velocity of flux	(kg/m^2s)
ρv	transverse mass velocity of flux	(kg/m^2s)
j	relative injection intensity	(-)
α	heat transfer coefficient	(W/m^2K)
γ	adiabatic exponent	(-)
R	radius	(m)
x	Cartesian coordinate	(m)
δ	thickness	(m)

SUBSCRIPTS

0	stagnation (total)
∞	free-stream
aw	adiabatic wall
w	wall
i	number
1	subsonic
2	supersonic
c	cold
h	hot
M	compressible

REFERENCES

[1] Goldstein, R.J., Kulkarni, K.S., “Energy separation in the wake of a cylinder,” *Journal of Heat Transfer*, 130(6), art. no. 061703, (2008).

[2] Van Oudheusden, B.W., “Energy separation in steady separated wake flow,” *Journal of Fluids Engineering*, *Transactions of the ASME,* 127(3), pp. 611-614, (2005).

[3] Han, B., Goldstein, R.J., “Instantaneous energy separation in a free jet - Part II. Total temperature measurement,” *International Journal of Heat and Mass Transfer*, 46(21), pp. 3983-3990, (2003).

[4] Han, B., Goldstein, R.J., Choi, H.G., “Energy separation in shear layers,” *International Journal of Heat and Mass Transfer*, 45 (1), pp. 47-55, (2001).

[5] O'Callaghan, J.J., Kurosaka, M., “Vortex-induced energy separation in shear flows,” *AIAA journal*, 31 (6), pp. 1157-1159, (1993).

[6] Ng, W.F., Chakroun, W.M., Kurosaka, M., “Time-resolved measurements of total temperature and pressure in the vortex street behind a cylinder,” *Physics of Fluids A*, 2 (6), pp. 971-976, (1990).

[7] Kurosaka, M., Gertz, J.B., Graham, J.E., Goodman, J.R., Sundaram, P., Riner, W.C., Kuroda, H., Hankey, W.L., “Energy separation in a vortex steet,” *Journal of Fluid Mechanics*, 178, pp. 1-29, (1987).

[8] Eckert, E.R.G., “Energy separation in fluid streams,” *International Communications in Heat and Mass Transfer*, 13 (2), pp. 127-143, (1986).

[9] Leont’ev, A.I., “Gas-dynamic methods of temperature stratification (a review),” *Fluid Dynamics* 37 (4), pp. 512-529, (2002).

[10] Burtsev, S.A., Leontiev, A.I., “Study of the influence of dissipative effects on the temperature stratification in gas flows (Review),“ *High Temperature*, 52(2), pp. 297–307, (2014).

[11] Hilsch, R., “The use of the expansion of gases in a centrifugal field as cooling process,” *Review of Scientific Instruments* 18 (2), 108–113, (1947).

[12] Xue, Y., Arjomandi, M., Kelso, R., “A critical review of temperature separation in a vortex tube,” *Experimental Thermal and Fluid Science*, 34 (8), pp. 1367-1374, (2010).

[13] Eiamsa-ard, S., Promvonge, P., “Review of Ranque-Hilsch effects in vortex tubes,” *Renewable and Sustainable Energy Reviews*, 12 (7), pp. 1822-1842, (2008).

[14] Sprenger, H., “Uber thermische Effekte in Resonanzrohren,” *Mitt. Inst. Aerodynamik*, 21, pp. 18-35, (1954).

[15] Raman, G., Srinivasan, K., “The powered resonance tube: From Hartmann's discovery to current active flow control applications,” *Progress in Aerospace Sciences*, 45 (4-5), pp. 97-123, (2009).

[16] Eliseev, Yu.B., Cherkez, A.Ya., “On the heating effect in gas flow over deep cavities,” *Fluid Dynamics*, 6 (3), pp. 368-377, (1971).

[17] /http://newmantools.com/vortex.com/

[18] Piralishvili, Sh.A., Polyaev, V.M., “Flow and thermodynamic characteristics of energy separation in a double-circuit vortex tube - an experimental investigation,” *Experimental Thermal and Fluid Science*, 12 (4), pp. 399-410, (1996).

[19] Brocher, E., Ardissone, J.-P., “Heating characteristics of a new type of Hartmann-Sprenger tube,” *International Journal of Heat and Fluid Flow*, 4 (2), pp. 97-102, (1983).

[20] Kadaba, P. V., Bondarenko, V.L., Arkharov, A.M., “Thermal characteristics of a Hartmann-Sprenger tube,” *International Journal of Refrigeration*, 13 (5), pp. 309-316, (1990).

[21] Leont’ev, A.I., “Gas-Dynamic methods of temperature stratification (a Review),” *Fluid Dynamics* 37 (4), pp. 512-529, (2002).

[22] Schlichting, H., *Boundary Layer Theory*, McGraw-Hill, New York (1968).

[23] Brinich, P., “Recovery temperatures and heat transfer near two-dimensional roughness elements at Mach 3.1,” *NACA Techn. Rep*. No. 4213 (1958).

[24] Leontiev, A.I., Vinogradov, Yu.A., Bednov, S.M., Golikov, A.N., Ermolaev, I.K., Dilevskaya, E.V., Strongin, M.M., “Effect of vortex flows at surface with hollow-type relief on heat transfer coefficients and equilibrium temperature in supersonic flow,” *Exp. Thermal Fluid Sci*. **26**, pp. 487-497 (2002).

[25] Titov, A.A., Leontiev, A.I., Vinogradov, U.A., Zditovets, A.G., Strongin, M.M., “Experimental investigation of skin friction drag and heat transfer on the surfaces with concavities in compressible fluid flow,” *Proceedings of14th International Heat Transfer Conference,* IHTC14-22585, 2, pp. 597-601, (2010).

[26] Kutateladze, S.S., Leontiev, A.I., “*Heat Transfer, Mass Transfer, and Friction in Turbulent Boundary Layers*,” Taylor and Francis New York (1990)

[27] Bartle, E.B, Leadon, B.M., “Experimental evaluation of heat transfer with transpiration cooling in a turbulent boundary layer at M= 3.2,” *J. Aerospace Sci*. 27, 78 (1960).

[28] Baryshev, Yu.V., Vinogradov, Yu. A., Leont’ev, A.I., Rozhdestvenskii, V.I., “Recovery factors for a permeable surface and a gas surface film in a supersonic turbulent boundary layer,” *Fluid Dynamics* 7(2), pp. 303-307 (1974).

[29] Yarygina, N.I. Heat transfer and friction in a compressible turbulent boundary layer on a permeable surface. *Candidate’s Dissertation in Technical Sciences*, Novosibirsk (1971).

[30] Leadon, B.M., Scott, C.J., “Transpiration cooling experiments in a turbulent boundary layer at M = 3,” *J. Aeronaut. Sci*. 23, pp. 798 (1956).

[31] M.W. Rubesin, C.C. Pappas, and A.F. Okuno, “The effect of fluid injection on the compressible turbulent boundary layer—preliminary tests on transpiration cooling of a plate at M= 2.7 with air as the injected gas,” *NACA RM A55119* (1955).

[32] Leont’ev, A.I., Lushchik, V.G., Yakubenko, A.E., “Temperature of a thermally-insulated permeable wall in a compressible flow,” *Fluid Dynamics* 43 (5), pp. 799-806 (2008).

[33] Burtsev, S.A., Leont’ev, A. I., “Temperature stratification in a supersonic gas flow,” *Izv. Ross. Akad. Nauk. Energetika* 5, pp. 101 (2000).

[34] Leont’ev, A.I., Lushchik, V.G., Yakubenko, A.E., “Injection/suction effect on energy separation in compressible flows,” *Fluid Dynamics* 46 (6), pp. 935-941 (2011).

[35] Makarov, M.S., Makarova, S.N., “Efficiency of energy separation at compressible gas flow in a planar duct,” *Thermophysics and Aeromechanics*, 20 (6), pp. 757-767, (2014).

[36] Vigdorovich, I.I., Leont'ev, A.I., “Energy separation of gases with low and high Prandtl numbers,” *Fluid Dynamics*, 48 (6), pp. 811-826, (2013).

[37] Vigdorovich, I.I., Leont'ev, A.I., “Theory of the energy separation of a compressible gas flow,” *Fluid Dynamics*, 45 (3), pp. 434-440, (2010).

[38] Volchkov, E.P., Makarov, M.S. “Gasdynamic temperature stratification in a supersonic flow,” *Izv. Ross. Akad. Nauk.* Energetika, 2, pp.19, (2006).

[39] Chirkin, V.S., *Thermal Properties of Materials* [in Russian], Fizmatgiz, Moscow (1959).

[40] Krzhizhanovskii, R.E., Shtern, Z.Yu., *Thermal Properties of Nonmetallic Materials (Oxides)* [in Russian], Energiya, Leningrad (1973).

[41] Petukhov, B.S., *Heat Transfer in a Single-Phase Medium in Motion. Laminar Boundary Layer,* [in Russian], Moscow Energy Institute, Moscow (1993).

[42] Matsuo, K., Miyazato, Y., Kim, H.-D. “Shock train and pseudo-shock phenomena in internal gas flows,” *Progress in Aerospace Sciences*, 35 (1), pp. 33-100, (1999).

[43] Vinogradov, Y.A., Zditovets, A.G., Strongin, M.M., “Experimental investigation of the temperature stratification of an air flow through a supersonic channel with a central body in the form of a porous permeable tube,” *Fluid Dynamics*, 48 (5), pp. 687-696, (2013).

[44] Shapiro, A. H., *The Dynamics and Thermodynamics of Compressible Fluid Flow*, Vol. 1 New York The Ronald Press Company (1953)